

# Direct stereochemical assignment of hexose and pentose residues in flavonoid O-glycosides by fast atom bombardment and electrospray ionization mass spectrometry<sup>†</sup>

Filip Cuyckens, Abdelaaty A. Shahat, Luc Pieters and Magda Claeys\*

Department of Pharmaceutical Sciences, University of Antwerp (UIA), Universiteitsplein 1, B-2610 Antwerp, Belgium

Received 21 May 2002; Accepted 24 October 2002

Mass spectrometric methods have been developed which allow the direct stereochemical assignment of terminal monosaccharide residues in flavonoid O-glycosides without the need for chemical hydrolysis. Standards containing a glucose, galactose, mannose, xylose, arabinose or apiose residue were examined because these monosaccharides are by far the most commonly encountered in flavonoid glycosides. Following acetylation, the major peracetylated sugar related fragments, generated by fast atom bombardment (FAB) or electrospray ionization (ESI), were selected for collisional activation employing a broad range of collision energies. Both FAB and ESI proved to be useful as ionization techniques. Stereoselective fragmentation was achieved and allowed us clearly to differentiate and characterize isomeric monosaccharide residues. The method developed was successfully applied to an unknown flavonoid containing a terminal pentose and hexose residue which was isolated from *Farsetia aegyptia*. Copyright © 2002 John Wiley & Sons, Ltd.

**KEYWORDS:** flavonoid glycosides; sugar residues; electrospray ionization; fast atom bombardment

## INTRODUCTION

Flavonoid glycosides are predominant forms of naturally occurring flavonoids in plants, representing a large group of secondary plant metabolites. They all contain a C<sub>15</sub> skeleton as an aglycone, are usually divided into O- and C-glycosyl flavonoids and are of interest because they have various biological activities, are useful for chemotaxonomy and are used as tracers in medicinal plant preparations.<sup>1,2</sup> Flavonoids generally occur as glycosides in plants because the effect of glycosylation renders the flavonoid less reactive and more water soluble, permitting storage of the flavonoids in the cell vacuole where they are mostly found. Glucose is by far the monosaccharide most commonly bound to flavonoids, whereas galactose, rhamnose, xylose and arabinose are not uncommon and mannose and apiose are also occasionally encountered.<sup>1</sup> Although <sup>1</sup>H and <sup>13</sup>C NMR techniques are preferred for stereochemical assignment, mass spectrometry (MS) can make a valuable contribution because it can be applied to much smaller quantities of isolated compounds. It provides the molecular mass, in addition to structural information on the flavonoid skeleton,<sup>3–15</sup> attachment points of carbohydrate residues to the aglycone,<sup>6–8</sup> the types of

carbohydrates present (mono-, di-, tri- or tetrasaccharides and hexoses, deoxyhexoses or pentoses)<sup>9–11</sup> and the type of interglycosidic linkages.<sup>12–15</sup> Early investigations of carbohydrates by means of MS analysis were performed by resorting to acetyl and methyl derivatives.<sup>16,17</sup> Derivatization of the compounds was required in order to obtain sufficient volatility necessary for electron ionization (EI) and chemical ionization (CI). Although more modern soft ionization techniques such as fast atom bombardment (FAB)<sup>18–20</sup> allow the detection of molecular ion species (i.e. protonated, deprotonated or sodiated species) of underivatized saccharides, Richter and co-workers<sup>21–24</sup> showed that acetylation can still be useful in the structural characterization of oligosaccharides and glycoside residues. It was demonstrated that the differentiation between a terminal glucose, galactose and mannose residue of naturally occurring glycosides could be achieved by low-energy collision-induced dissociation (CID) using a triple-quadrupole mass spectrometer equipped with a CI source. In this study, we followed the same approach for developing methodology to differentiate and characterize the terminal monosaccharide residue of flavonoid O-glycosides. Standards containing the major hexoses and pentoses found attached to flavonoids were analyzed utilizing FAB and electrospray ionization (ESI). Deoxyhexoses were not included in this study because, to our knowledge, only rhamnose occurs in association with flavonoids and can easily be distinguished from pentoses and hexoses by its different mass. Finally, the monosaccharide residues of an unknown flavonoid, isolated

\*Correspondence to: Magda Claeys, Department of Pharmaceutical Sciences, University of Antwerp (UIA), Universiteitsplein 1, B-2610 Antwerp, Belgium. E-mail: claeys@uia.ua.ac.be

<sup>†</sup>Paper presented at the 20th Informal Meeting on Mass Spectrometry, Fiera di Primiero, Italy, 12–16 May 2002.

from *Farsetia aegyptia*, containing a terminal pentose and hexose, were characterized using the method developed.

## EXPERIMENTAL

### Materials

Quercetin-3-*O*- $\beta$ -D-glucopyranoside (isoquercitrin), quercetin-3-*O*- $\beta$ -D-galactopyranoside (hyperoside), quercetin-4'-*O*- $\beta$ -D-glucopyranoside (spiraeoside), syringetin-3-*O*- $\beta$ -D-glucopyranoside, syringetin-3-*O*- $\beta$ -D-galactopyranoside, quercetin-3-*O*- $\alpha$ -L-arabinopyranosyl-(1  $\rightarrow$  6)- $\beta$ -D-glucopyranoside (peltatoside) and apigenin-7-*O*- $\beta$ -D-apiofuranosyl-(1  $\rightarrow$  2)- $\beta$ -D-glucopyranoside (apiin) were obtained from Extrasynthèse (Genay, France). Because flavonoids containing a xylose or mannose residue are commercially unavailable, 4-*O*- $\beta$ -D-xylopyranosyl- $\beta$ -D-xylopyranose (xylobiose) and 3-*O*- $\alpha$ -D-mannopyranosyl- $\alpha$ -D-mannopyranose (mannobiose) were used instead. They were both purchased from Sigma (St. Louis, MO, USA). The structures of the monosaccharide residues examined are shown in Fig. 1. All compounds were acetylated overnight at room temperature with pyridine-acetic anhydride (1:1, v/v). The unknown flavonoid was isolated from the leaves of *Farsetia aegyptia* (full details will be reported elsewhere) and its complete structure was elucidated by the combined use of NMR and MS methods.

### Mass spectrometry

Mass spectrometric data were obtained on an Autospec-*oa*-ToF mass spectrometer (Micromass, Manchester, UK) with an EBE-*oa*-time-of-flight configuration equipped with a cesium ion source. The acronym FAB is used throughout to refer to cesium ion bombardment. The acceleration voltage in the source was 8 kV. The samples were dissolved in methanol (10  $\mu$ g  $\mu$ l<sup>-1</sup>) and 1  $\mu$ l of the solution was mixed with 2  $\mu$ l of the liquid matrix on the stainless-steel probe. Glycerol and 3-nitrobenzyl alcohol were tested as matrices. Glycerol resulted in a better signal-to-noise ratio and was employed in subsequent experiments. High-energy CID spectra were obtained using linked scanning at constant *B/E* with helium as collision gas until 50% attenuation of the precursor ion beam. In the tandem mass spectrometric (MS/MS) mode precursor ions were selected by MS1 (EBE configuration) and, after passing the collision cell, product ions were recorded on the microchannel plate detector of the time-of-flight analyzer. The collision cell was floated at 200,

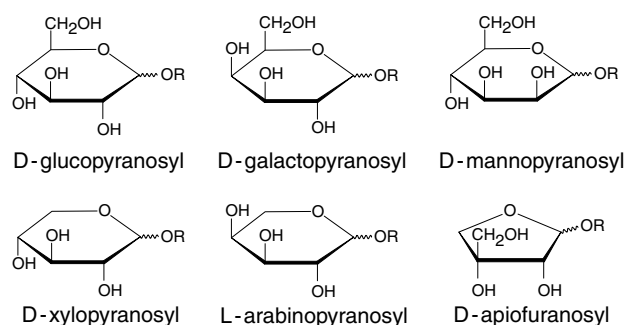


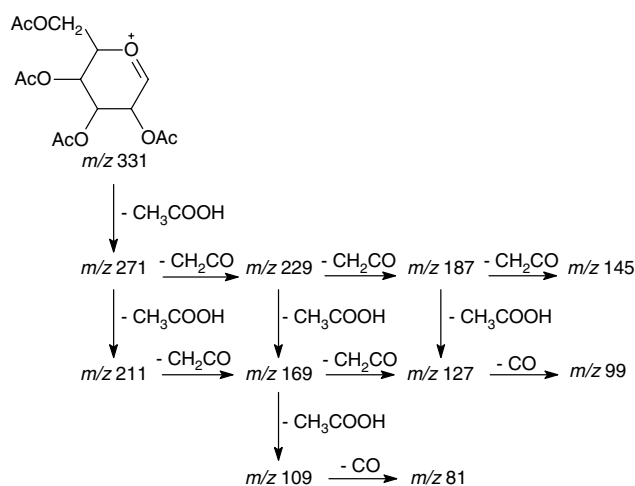
**Figure 1.** Structures of the monosaccharides studied.

400 or 800 V and helium, methane or xenon was used as the collision gas until the precursor ion beam was reduced to 50% of its original value. Using this approach, a wide range of collision energies could be used.

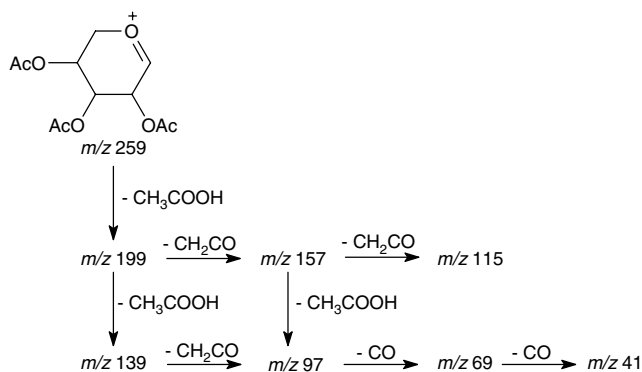
ESI spectra were acquired on the same instrument. The ESI source was operated at 4 kV. The acetylated compounds were dissolved in water-methanol (1:1, v/v) at a concentration of 100  $\mu$ M. They were introduced into the ESI source by a syringe pump (Model 22 syringe infusion pump, Harvard Apparatus, South Natick, MA, USA) employing a 500  $\mu$ l syringe (Hamilton, Reno, NV, USA) at a constant flow-rate of 5  $\mu$ l min<sup>-1</sup>. Nitrogen was used as both bath gas (80 °C) and nebulizing gas. The effect of the cone voltage on the ionization was examined. Product ion tandem mass spectra using low- and high-energy CID were recorded as done in the case of ionization by FAB. Data acquisition and processing were performed using OPUS V3.1X software. All scans were acquired in the continuum mode. The nomenclature proposed by Domon and Costello<sup>25</sup> for glycoconjugates was adopted to denote the fragment ions. If the charge is retained on the carbohydrate residue, fragments are designated as <sup>k,l</sup>A<sub>i</sub>, B<sub>i</sub> and C<sub>i</sub>, where *i* represents the number of the glycosidic bond cleaved counting from the non-reducing terminus and the superscripts *k* and *l* indicate the cleavages within the carbohydrate rings.

## RESULTS AND DISCUSSION

Saccharidic fragment ions are rarely seen in first-order spectra of underivatized flavonoids because the charge generally stays associated with the aglycone part.<sup>9-15</sup> By acetylating flavonoid *O*-glycosides, peracetylated sugar related fragment ions are also detected with a high relative abundance and can readily be selected for further CID experiments. The fragmentation pathways of the peracetylated hexose and pentose residues are shown in Schemes 1 and 2, respectively. They relate mainly to the loss of acetic acid (60 u) and of ketene (42 u). The latter process seems to be facilitated if preceded by loss of acetic acid and if the acetyl groups involved are in a 1,2- or a 1,3-relationship.<sup>16,26,27</sup>



**Scheme 1.** Fragmentation pathways of the B<sub>1</sub><sup>+</sup> ion of peracetylated hexose-containing compounds.



**Scheme 2.** Fragmentation pathways of the  $B_1^+$  ion of peracetylated pentose-containing compounds.

## Hexoses

### Fast atom bombardment

The first-order FAB spectra of the peracetylated flavonoid-glycosides examined reveal, along with the peracetylated sugar fragment ion ( $B_1^+$ ), nearly all major sugar fragments listed in Scheme 1. Although most of them have a high relative abundance, we found it almost impossible to distinguish the different hexose residues in a reproducible way. Therefore, CID experiments were performed on all the major sugar fragments to reveal differences in fragmentation behavior between the three hexose residues investigated.

According to Richter and co-workers,<sup>21</sup> the ease of differentiation between hexose residues depends on the collision energy employed and an optimum for distinction is readily attained at lower collision energies. Product ion tandem mass spectra were recorded at different collision energies by changing the collision gas and the voltage of the collision cell. Selection of the peracetylated hexose fragment ( $B_1^+$ ) at  $m/z\ 331$  did not result in the expected difference in  $[m/z\ 127]/[m/z\ 109]$  ratios as described by Richter and co-workers.<sup>21</sup> However, a  $[B_1 - \text{CH}_3\text{COOH}]^+$  fragment ion at  $m/z\ 271$  was visible in all the spectra of peracetylated glucose and mannose derivatives independently of the collision energy used, whereas it was hardly seen, if at all, in the spectra of peracetylated galactose derivatives. The intensity of the peak at  $m/z\ 271$  exceeded that at  $m/z\ 229$  for glucose and mannose, whereas the peak at  $m/z\ 229$  was more intense in the case of a galactose residue. The differentiation based on the relative abundance of the  $m/z\ 271$  fragment ion is even more straightforward using  $B/E$  linked scanning, where  $[B_1 - \text{CH}_3\text{COOH}]^+$  at  $m/z\ 271$  is the most abundant product ion for glucose, whereas it is a minor product for galactose and has an intermediate relative abundance for mannose (Fig. 2).

Another way to differentiate clearly between hexose residues can easily be made by CID of the  $[B_1 - 2\text{CH}_3\text{COOH} - 2\text{CH}_2\text{CO}]^+$  ion at  $m/z\ 169$ . Figure 3 illustrates the low-energy CID spectra obtained for the monosaccharide fragment at  $m/z\ 169$  using helium as collision gas. The  $[B_1 - 2\text{CH}_3\text{COOH} - 2\text{CH}_2\text{CO}]^+$  ion at  $m/z\ 127$  has a higher relative abundance than the  $[B_1 - 3\text{CH}_3\text{COOH} - \text{CH}_2\text{CO}]^+$  ion at  $m/z\ 109$  for galactose, whereas the opposite holds for a mannose and glucose residue. The same peak intensity

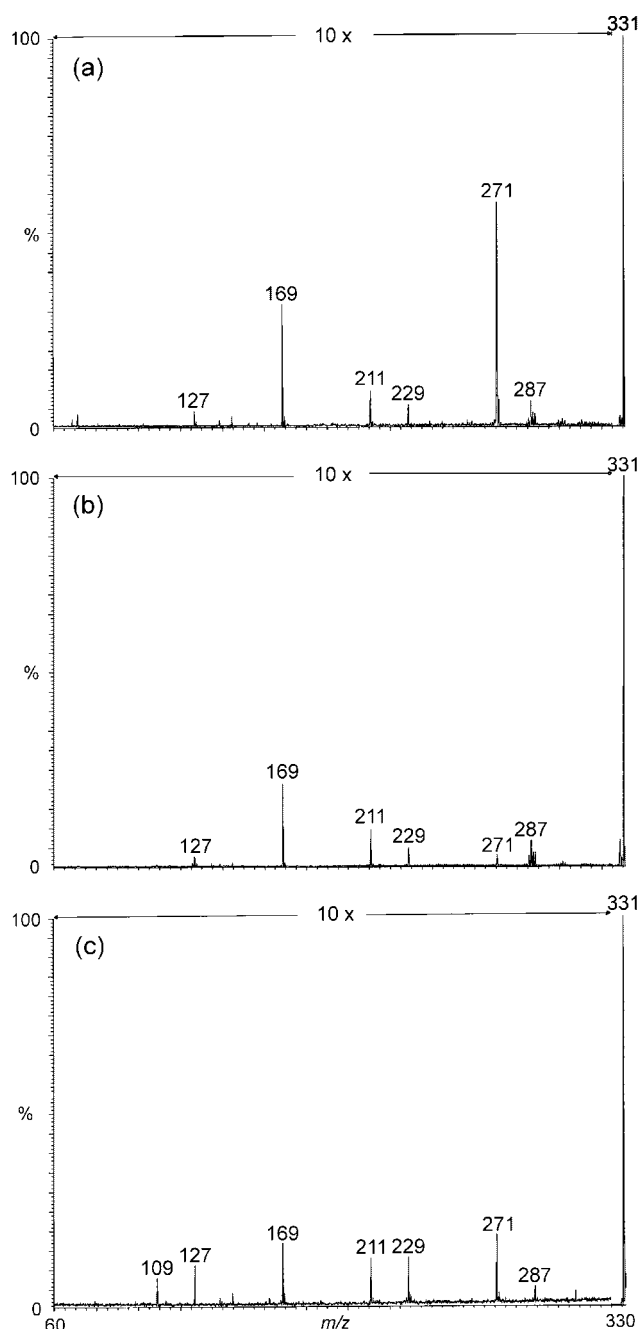


**Figure 2.** High-energy CID spectra of the peracetylated  $B_1^+$  ion of (a) glucose-, (b) galactose- and (c) mannose-containing compounds (isoquercitrin, hyperoside and mannobiose, respectively) generated by FAB using linked scanning at constant  $B/E$  and helium as collision gas.

ratios are obtained for the whole range of collision energies applied, indicating that this method is robust.

The spectra obtained for the  $B_1^+$  and  $[B_1 - 2\text{CH}_3\text{COOH} - 2\text{CH}_2\text{CO}]^+$  ions of peracetylated quercetin-4'- $O$ - $\beta$ -D-glucopyranoside, syringetin-3- $O$ - $\beta$ -D-glucopyranoside and syringetin-3- $O$ - $\beta$ -D-galactopyranoside were similar to those illustrated for their glucose and galactose analogues, quercetin-3- $O$ - $\beta$ -D-glucopyranoside and quercetin-3- $O$ - $\beta$ -D-galactopyranoside (Figs 2 and 3).

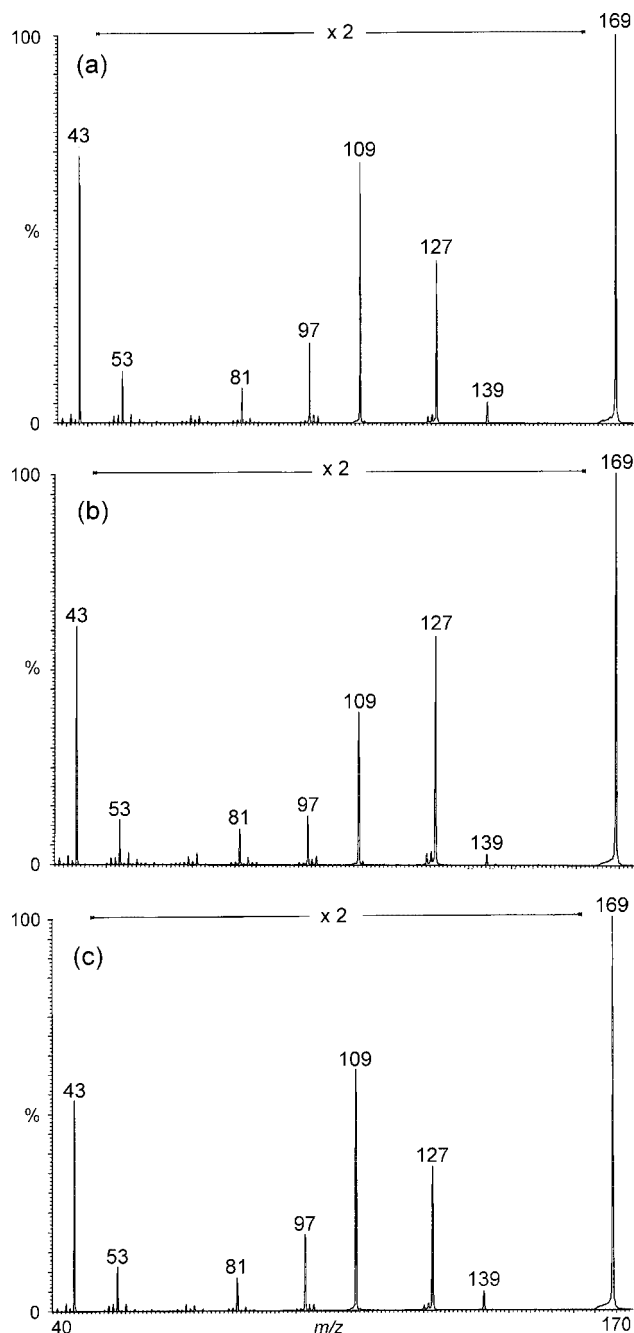


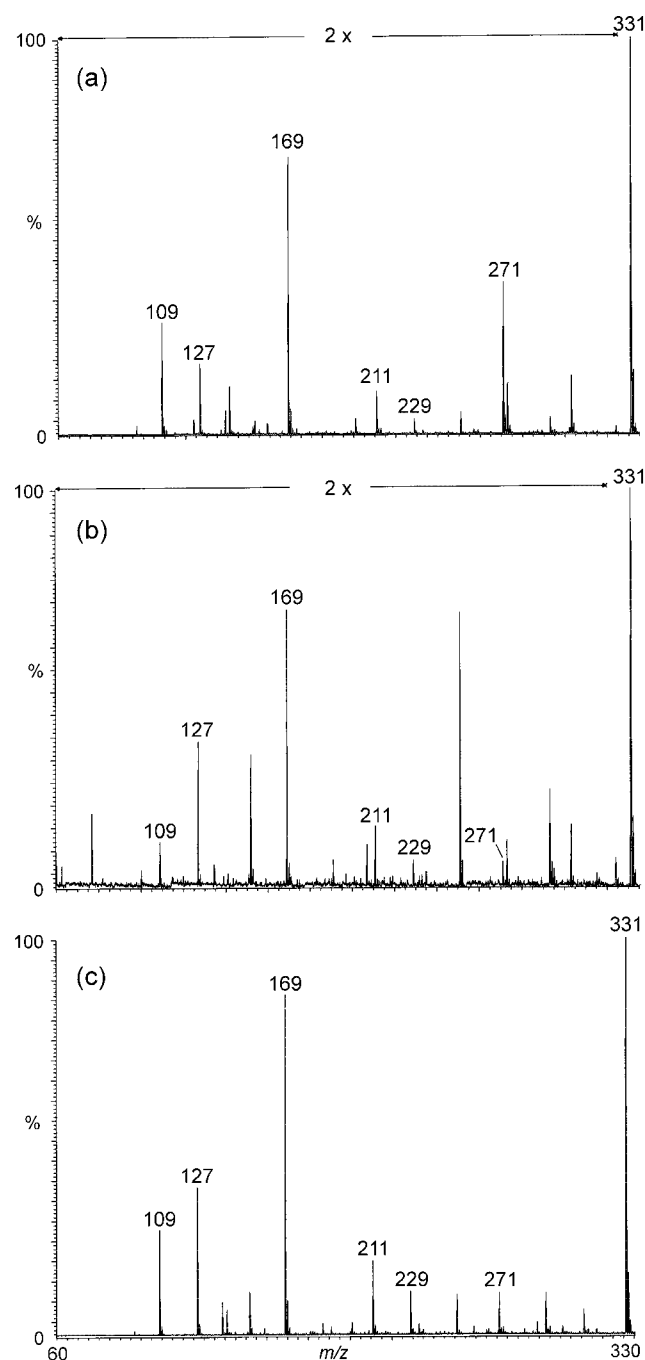
**Figure 3.** Low-energy CID spectra obtained for the  $[B_1 - 2CH_3COOH - 2CH_2CO]^+$  fragment at  $m/z$  169 of (a) glucose-, (b) galactose- and (c) mannose-containing compounds (isoquercitrin, hyperoside and mannoibiose, respectively) generated by FAB.

#### Electrospray ionization

ESI mass spectra were examined over the full range of cone voltages (0–250 V). Above a cone voltage of 75 V, a  $B_1^+$  ion at  $m/z$  331 becomes clearly visible. On further increasing the cone voltage, CID-like processes occur in the ion source, giving rise to all major sugar related fragments and are as such providing structure information. Figure 4 shows the lower mass range of the first-order ESI spectra acquired at a cone voltage of 200 V. The higher relative abundance of the ion at  $m/z$  109 compared with that at  $m/z$  127 and the more abundant fragment at  $m/z$  271 for glucose (Fig. 4(a)) in

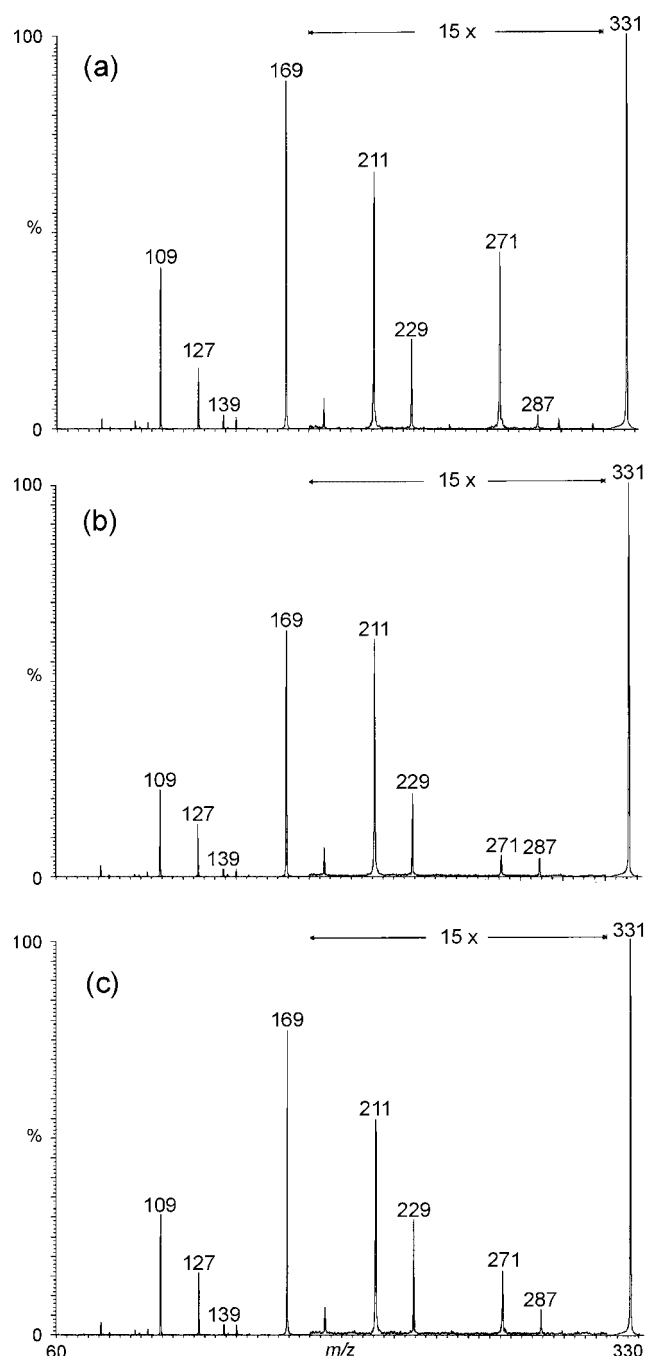
comparison with galactose (Fig. 4(b)) are consistent with the behavior discussed previously for FAB. The ESI spectrum illustrated in Fig. 4(c) for peracetylated mannose shows an intermediate behavior that is closer to that of galactose. This technique should be used with caution because the relative abundance of the ions can change considerably with increasing cone voltage. In our experience, higher cone voltages (200–250 V) are to be preferred because they result in the clearest differentiation and the highest sensitivity and reproducibility.

Figure 5 illustrates the low-energy CID spectra of peracetylated  $B_1^+$ . The loss of one acetic acid residue is relatively



**Figure 4.** Lower mass range of the first-order ESI spectra of peracetylated (a) isoquercitrin, (b) hyperoside and (c) mannoibiose acquired at higher cone voltage (200 V).

more pronounced for glucose, resulting in an ion with higher relative abundance at  $m/z$  271 compared with that at  $m/z$  229, whereas the opposite holds for galactose and mannose. Hence, as noted in the first-order ESI spectra, the fragmentation of mannose follows more closely that of galactose and is in contrast with observations in FAB. However, the peak intensity ratios between  $[m/z\ 271]/[m/z\ 229]$  and  $[m/z\ 271]/[m/z\ 211]$  differ sufficiently to distinguish both hexose residues. The values were  $4.5 \pm 0.6$  ( $[m/z\ 229]/[m/z\ 271]$ ) and  $10.5 \pm 0.9$  ( $[m/z\ 211]/[m/z\ 271]$ ) for galactose, whereas they were  $1.5 \pm 0.3$  ( $[m/z\ 229]/[m/z\ 271]$ ) and  $3.1 \pm 0.3$  ( $[m/z\ 211]/[m/z\ 271]$ ) for mannose.



**Figure 5.** Low-energy CID spectra obtained for the peracetylated  $B_1^+$  ion of (a) isoquercitrin, (b) hyperoside and (c) mannobiose generated by ESI using helium as collision gas.

Product ion tandem mass spectra of the  $[B_1 - 2CH_3COOH - 2CH_2CO]^+$  ion at  $m/z$  169 were also obtained (results not shown). Whereas in FAB the  $m/z$  109 ion was the most abundant fragment for glucose and mannose (Fig. 3), the  $m/z$  127 ion was always much more abundant than the  $m/z$  109 ion in the product ion tandem mass spectra of the  $m/z$  169 ion generated in ESI. Different  $[m/z\ 127]/[m/z\ 109]$  peak intensity ratios were also obtained in ESI for the three epimers studied, but these differences are rather small; the relative abundance of the  $m/z$  127 ion increases slightly with increasing cone voltage, making the determination of the hexose residue uncertain.

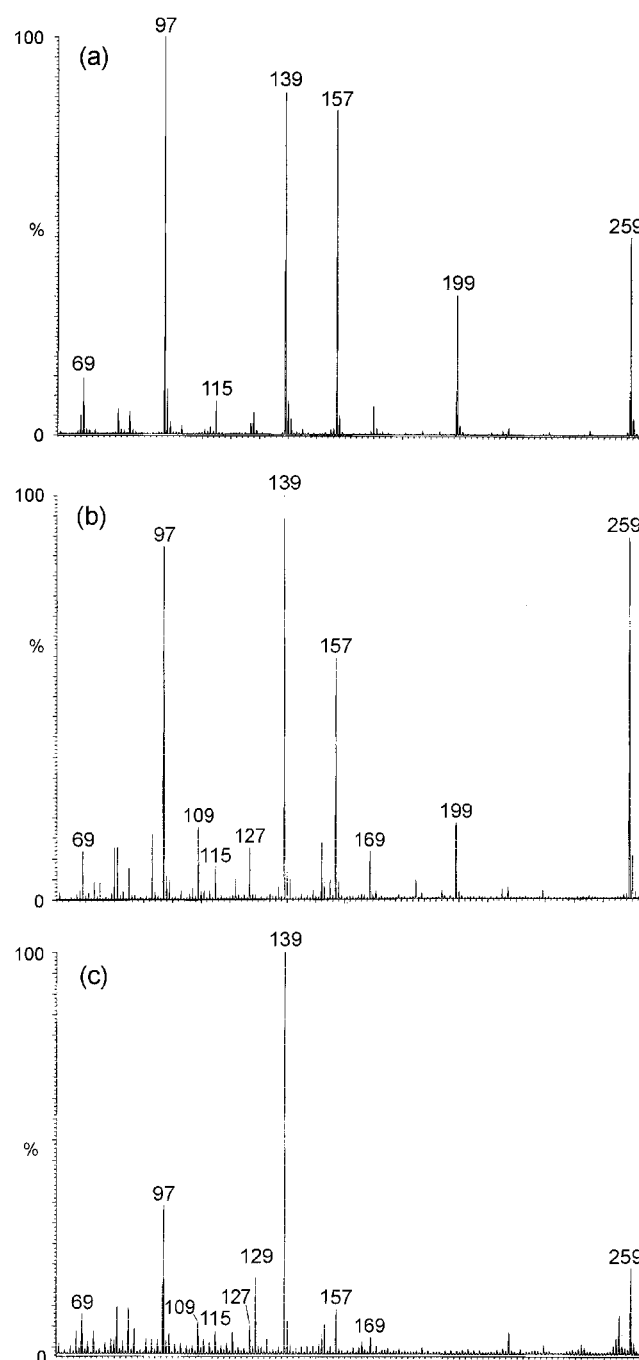


**Figure 6.** Lower mass range of the first-order FAB spectra of peracetylated (a) xylobiose, (b) peltatoside and (c) apiin.

## Pentoses

### Fast atom bombardment

Figure 6 illustrates the lower mass range of the first-order FAB spectra of the peracetylated pentose-containing compounds, xylobiose, peltatoside and apiin. The relative abundance of the  $[B_1 - 2CH_3COOH]^+$  ion at  $m/z$  139 can be compared with that of the  $m/z$  97, 157, 199 and 259 ions to differentiate and characterize the three pentose residues (Table 1). Especially the  $[m/z$  139]/ $[m/z$  199] peak intensity ratios are strikingly different. The relative abundance of the  $m/z$  199 ion  $[B_1 - CH_3COOH]^+$  follows the order xylose > arabinose > apiose. The more abundant  $[B_1 - CH_3COOH]^+$  ion for xylobiose compared with peltatoside is in full agreement with observations made for the hexoses ( $m/z$  271) and as expected because the structure of xylose is stereochemically similar to that of glucose whereas arabinose is similar to galactose (Fig. 1). It has been reported by Blok-Tip *et al.*<sup>28</sup> that the decomposition of the  $[B_1 - CH_3COOH]^+$  ion proceeds to a greater extent for ribofuranose than ribopyranose. This could also partly explain the different ratios observed because apiose is in the furanose form whereas xylose and arabinose are in the pyranose form. Another characteristic of the apiose derivative apiin is a  $[B_1 - CH_3COOH - CH_2CO - CO]^+$  ion at  $m/z$  129 that was absent for the xylose- and arabinose-containing compounds, xylobiose and peltatoside.

The same observations were made for the product ion tandem mass spectra of the peracetylated  $B_1^+$  ion at  $m/z$  259 (Table 1). The product ion tandem mass spectra are very similar to the spectra for the  $B_1^+$  ion generated by ESI (Fig. 7). Both low- and high-energy CID can be used but the collision energy should be kept constant because the relative abundances and peak intensity ratios change with increasing collision energy.

Similar tendencies can also be noted using linked scanning at constant  $B/E$  value (results not shown). The  $[B_1 - CH_3COOH]^+$  fragment is absent for the apiose derivative apiin, whereas it is the major fragment for the xylose- and arabinose-containing compounds xylobiose and peltatoside. The fragments at  $m/z$  139 and 157 have a larger relative

abundance than the  $m/z$  199 ion in the spectrum of arabinose compared with xylose where the  $m/z$  139 peak has a negligible relative abundance.

The first-order FAB spectra of peltatoside and apiin show additional fragments at  $m/z$  109, 127, 169 and 271 (Fig. 6). These hexose-related fragments originate from the internal glucose present in the disaccharide moiety. The  $m/z$  169 product ion spectrum (not shown) revealed an  $[m/z$  127]/ $[m/z$  109] ratio identical with that shown in Fig. 3(a) for the  $m/z$  169 fragment of peracetylated isoquercitrin.

### Electrospray ionization

At cone voltages exceeding 100 V the  $B_1^+$  ion at  $m/z$  259 appears, accompanied by other sugar-related fragments. A further increase in the cone voltage reveals all major fragments. Apiose can easily be recognized because only the  $[B_1 - 2CH_3COOH]^+$  fragment at  $m/z$  139 can be detected. For peracetylated xylose and arabinose also fragments at  $m/z$  157 and 199 can be found but their peak intensity ratios fluctuate considerably when the cone voltage increases, making the distinction between the two epimers hard to accomplish.

Figure 7 shows the low-energy CID spectra obtained for the peracetylated  $B_1^+$  ion at  $m/z$  259 using helium as collision gas. Again, apiose can clearly be identified because the fragment at  $m/z$  199 is virtually absent and the signal intensity of  $m/z$  157 low ( $[m/z$  139]/ $[m/z$  157] =  $13.3 \pm 0.5$ ). Another characteristic is that an additional  $[B_1 - CH_3COOH - CH_2CO - CO]^+$  fragment at  $m/z$  129 can only be seen in the spectrum of peracetylated apiose. The relative abundances of the fragments at  $m/z$  139, 157 and 199 can be used to differentiate between an arabinose ( $[m/z$  139]/ $[m/z$  199] =  $10.4 \pm 2.0$ ;  $[m/z$  139]/ $[m/z$  157] =  $3.7 \pm 0.8$ ) and a xylose ( $[m/z$  139]/ $[m/z$  199] =  $3.5 \pm 0.3$ ;  $[m/z$  139]/ $[m/z$  157] =  $1.6 \pm 0.1$ ) residue. The values given here were obtained using helium as collision gas, but similar results were also found with xenon.

### Application to an unknown flavonoid isolated from *Farsetia aegyptia*

An unknown flavonoid, isolated from the leaves of *Farsetia aegyptia*, was characterized by mass spectrometric

**Table 1.** Mass spectral data obtained by FAB: relative abundances were obtained by averaging the values from three different analyses on three different days

Spectra	Compound	$m/z$					$m/z$	$m/z$	$m/z$	$m/z$
		259	199	157	139	97	139/259	139/199	139/157	139/97
FAB <sup>a</sup>	Xylose	55.3 ± 6.8	40.2 ± 5.6	76.7 ± 5.3	93.3 ± 7.0	99.6 ± 0.7	1.7 ± 0.1	2.3 ± 0.2	1.2 ± 0.1	0.9 ± 0.1
	Arabinose	81.7 ± 7.6	18.1 ± 0.9	58.1 ± 1.1	100	91.9 ± 6.5	1.2 ± 0.1	5.6 ± 0.3	1.7 ± 0.1	1.1 ± 0.1
	Apiose	35.7 ± 8.1	5.8 ± 2.6	14.6 ± 2.3	100	38.2 ± 7.9	2.9 ± 0.6	20.8 ± 12.3	7.0 ± 1.1	2.7 ± 0.5
He <sup>b</sup>	Xylose	100	16.5 ± 4.6	25.2 ± 2.4	51.5 ± 4.2	69.2 ± 5.0	0.5 ± 0.0	3.2 ± 0.6	2.1 ± 0.1	0.7 ± 0.1
	Arabinose	100	12.1 ± 4.1	17.9 ± 0.9	69.8 ± 13.8	65.6 ± 10.7	0.7 ± 0.1	6.0 ± 1.1	3.9 ± 0.8	1.1 ± 0.4
	Apiose	100	0.8 ± 0.2	6.7 ± 1.2	59.2 ± 3.4	24.0 ± 3.5	0.6 ± 0.0	79.5 ± 15.8	9.1 ± 1.8	2.5 ± 0.4
Xe <sup>c</sup>	Xylose	100	12.3 ± 2.1	10.3 ± 1.0	21.0 ± 0.3	18.2 ± 2.9	0.2 ± 0.0	1.6 ± 0.4	2.1 ± 0.2	1.2 ± 0.2
	Arabinose	100	6.1 ± 1.3	7.2 ± 1.3	19.7 ± 1.6	12.1 ± 0.9	0.2 ± 0.0	3.4 ± 0.8	2.8 ± 0.5	1.7 ± 0.1
	apiose	100	1.3 ± 0.7	1.4 ± 0.4	26.1 ± 1.5	5.4 ± 0.2	0.3 ± 0.0	26.1 ± 16.2	19.7 ± 6.8	4.9 ± 0.2

<sup>a</sup> FAB: first-order FAB spectra of the peracetylated flavonoid O-glycosides.

<sup>b</sup> He: low-energy CID spectra of peracetylated  $B_1^+$  using helium as collision gas.

<sup>c</sup> Xe: high-energy CID spectra of peracetylated  $B_1^+$  using xenon as collision gas.

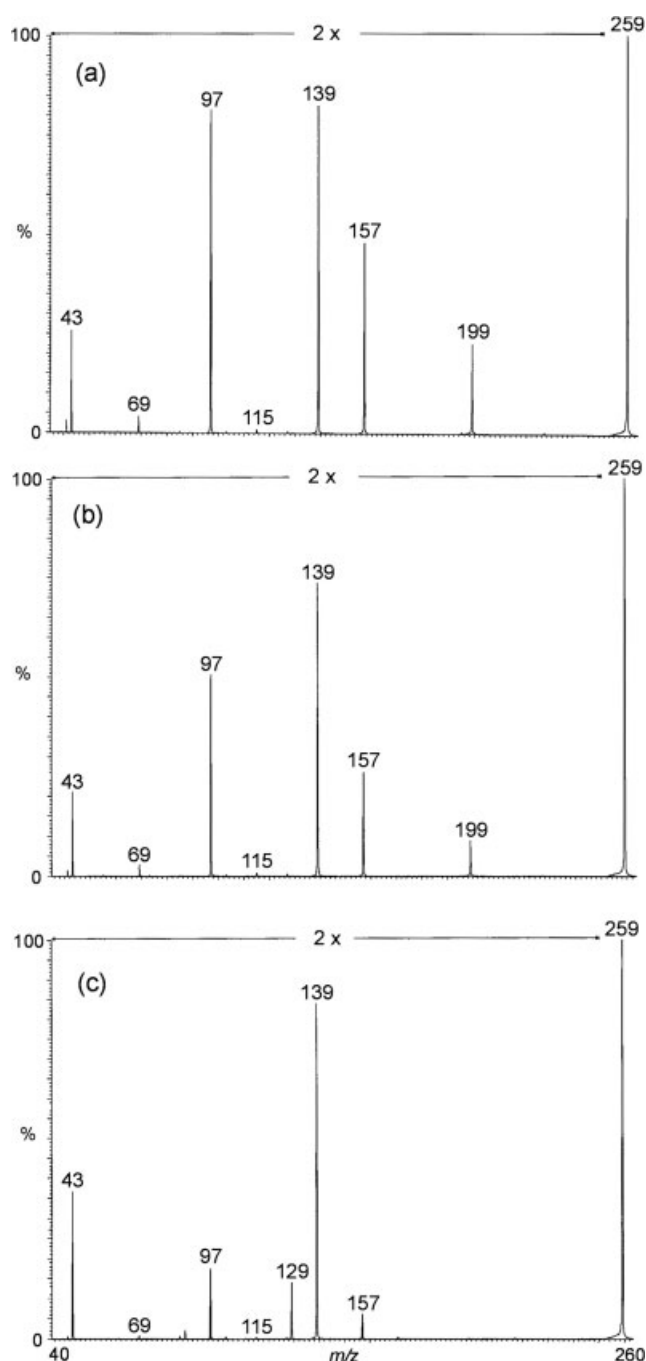


**Figure 7.** Low-energy CID spectra obtained for the peracetylated  $B_1^+$  ion of (a) xylobiose, (b) peltatoside and (c) apiin generated by ESI using helium as collision gas.

approaches as isorhamnetin-3-*O*-pentoside-7-*O*-hexosyl-rhamnoside. The compound was peracetylated and the methods developed in this work were applied to define the pentose and hexose residues. The peracetylated monosaccharide ions ( $B_1^+$ ) at  $m/z$  259 for the pentose and at  $m/z$  331 for the hexose were clearly visible in the first-order ESI spectrum. The low-energy CID spectrum of peracetylated  $B_1^+$  at  $m/z$  331 revealed a glucose structure for the hexose because the peak intensity of the  $[B_1 - CH_3COOH]^+$  ion at  $m/z$  271 was significantly higher than that of the ion at  $m/z$  229 (see Fig. 5). From the peak intensity ratios observed in the low- and high-energy CID spectra of the peracetylated  $B_1^+$  ion at  $m/z$  259,

an arabinose residue identity could be inferred. The values were  $12.0 \pm 6.6$  ( $[m/z 139]/[m/z 199]$ ) and  $3.3 \pm 0.3$  ( $[m/z 139]/[m/z 157]$ ) using helium as collision gas and  $6.8 \pm 1.7$  ( $[m/z 139]/[m/z 199]$ ) and  $2.7 \pm 1.2$  ( $[m/z 139]/[m/z 157]$ ) using xenon as collision gas. All values correspond within the standard deviation of those obtained for arabinose. Taking these results into account, the structure of the unknown flavonoid was defined as isorhamnetin-3-*O*-arabinoside-7-*O*-glucosylrhamnoside. Subsequently, the structure was confirmed and completed (i.e. with a 1,2-linkage between the rhamnose and glucose residues) by NMR spectroscopy.

## CONCLUSIONS

Both FAB and ESI in combination with CID have been shown to be useful for the direct stereochemical assignment of hexose and pentose residues in acetylated flavonoid *O*-glycosides. The differentiation between a glucose and a galactose residue can easily be made by employing the  $[m/z 127]/[m/z 109]$  peak intensity ratios and the relative abundance of the  $[B_1 - CH_3COOH]^+$  fragment at  $m/z$  271. Mannose shows intermediate relative abundances and behaves in FAB more like glucose, whereas in ESI the behavior is more similar to that observed for galactose. For the three pentoses considered in this study, stereoselective fragmentation was observed in the first-order FAB spectra and in the product ion CID spectra of the peracetylated  $B_1^+$  ion at  $m/z$  259 generated by FAB or ESI. The  $[B_1 - 2CH_3COOH]^+$  fragment at  $m/z$  139 revealed a different relative abundance to those of the other sugar fragments for the pentoses examined. Especially the  $[m/z 139]/[m/z 199]$  peak intensity ratios are strikingly different, showing the order apiose > arabinose > xylose. Apiose can also be recognized by the presence of an additional  $[B_1 - CH_3COOH - CH_2CO - CO]^+$  fragment at  $m/z$  129.

The methodology developed in this study is not restricted to flavonoid *O*-glycosides and has also been successfully applied to non-flavonoids (i.e. phytosterol *O*-glycosides), but it should be mentioned that other monosaccharide residues not included in this study can be encountered.

## Acknowledgements

We acknowledge the financial support by the Fund for Scientific Research (Belgium–Flanders; FWO; grant No. 6.0082.98) and the Concerted Actions of the Regional Government of Flanders (grant No. 99/3/34). F. Cuyckens thanks the Vlaams Instituut voor de Bevordering van het Wetenschappelijk-Technologisch Onderzoek in de Industrie (IWT) for a doctoral fellowship.

## REFERENCES

1. Markham KR. *Techniques of Flavonoid Identification*. Academic Press: London, 1982.
2. Harborne JB. *The Flavonoids: Advances in Research Since 1986*. Chapman and Hall: London, 1994.
3. Ma YL, Li QM, Van den Heuvel H, Claeys M. *Rapid Commun. Mass Spectrom.* 1997; **11**: 1357.
4. Wolfender JL, Waridel P, Ndjoko K, Hobby KR, Major HJ, Hostettmann K. *Analisis* 2000; **28**: 895.
5. Fabre N, Rustan I, de Hoffmann E, Quetin-Leclercq J. *J. Am. Soc. Mass Spectrom.* 2001; **12**: 707.
6. Sakushima A, Nishibe S, Takeda T, Ogihara Y. *Mass Spectroscopy* 1988; **36**: 71.

7. Becchi M, Fraisse D. *Biomed. Mass Spectrom.* 1989; **18**: 122.
8. Li QM, Van den Heuvel H, Dillen L, Claeys M. *Biol. Mass Spectrom.* 1992; **21**: 213.
9. Sakushima A, Nishibe S. *Phytochemistry* 1988; **27**: 915.
10. Sägesser M, Deinzer M. *J. Am. Soc. Brew. Chem.* 1996; **54**: 129.
11. Häkkinen S, Auriola S. *J. Chromatogr. A* 1998; **829**: 91.
12. Careri M, Elviri L, Mangia A. *Rapid Commun. Mass Spectrom.* 1999; **13**: 2399.
13. Ma YL, Cuyckens F, Van den Heuvel H, Claeys M. *Phytochem. Anal.* 2001; **12**: 159.
14. Satterfield M, Brodbelt JS. *J. Am. Soc. Mass Spectrom.* 2001; **12**: 537.
15. Cuyckens F, Rozenberg R, de Hoffmann E, Claeys M. *J. Mass Spectrom.* 2001; **36**: 1203.
16. Biemann K, De Jongh DC, Schnoes KH. *J. Am. Chem. Soc.* 1963; **85**: 1763.
17. De Jongh DC, Biemann K. *J. Am. Chem. Soc.* 1963; **85**: 2289.
18. Dallinga JW, Heerma W. *Biomed. Environ. Mass Spectrom.* 1989; **18**: 363.
19. Garozzo D, Giuffrida M, Impallomeni G, Ballistreri A, Montaudou G. *Anal. Chem.* 1990; **62**: 279.
20. Dallinga JW, Heerma W. *Biol. Mass Spectrom.* 1991; **20**: 215.
21. Müller DR, Domon B, Blum W, Raschdorf F, Richter WJ. *Biomed. Environ. Mass Spectrom.* 1988; **15**: 441.
22. Domon B, Müller DR, Richter WJ. *Org. Mass Spectrom.* 1989; **24**: 357.
23. Domon B, Müller DR, Richter WJ. *Biomed. Environ. Mass Spectrom.* 1990; **19**: 390.
24. Vouros P, Müller DR, Richter WJ. *J. Mass Spectrom.* 1999; **34**: 346.
25. Domon B, Costello CE. *Glycoconj. J.* 1988; **5**: 397.
26. Radford T, DeJongh DC. In *Biochemical Applications in Mass Spectrometry*, Waller GR (ed.). Wiley: New York, 1972; 313.
27. Kováčik V, Petráková E, Mihálov V, Tvaroška I, Heerma W. *Biomed. Mass Spectrom.* 1985; **2**: 49.
28. Blok-Tip L, Heerma W, Haverkamp J. *Org. Mass Spectrom.* 1993; **28**: 139.